

Analytical Methods

Accepted Manuscript



This is an *Accepted Manuscript*, which has been through the Royal Society of Chemistry peer review process and has been accepted for publication.

Accepted Manuscripts are published online shortly after acceptance, before technical editing, formatting and proof reading. Using this free service, authors can make their results available to the community, in citable form, before we publish the edited article. We will replace this *Accepted Manuscript* with the edited and formatted *Advance Article* as soon as it is available.

You can find more information about *Accepted Manuscripts* in the [Information for Authors](#).

Please note that technical editing may introduce minor changes to the text and/or graphics, which may alter content. The journal's standard [Terms & Conditions](#) and the [Ethical guidelines](#) still apply. In no event shall the Royal Society of Chemistry be held responsible for any errors or omissions in this *Accepted Manuscript* or any consequences arising from the use of any information it contains.

1
2
3
4
5
6
7
8
9
10
11
12
13
14
15
16
17
18
19
20
21
22
23
24
25
26
27
28
29
30
31
32
33
34
35
36
37
38
39
40
41
42
43
44
45
46
47
48
49
50
51
52
53
54
55
56
57
58
59
60

Electrochemical sensing of paracetamol and its simultaneous resolution in the presence of dopamine and folic acid at multi-walled carbon nanotubes/poly(glycine) composite modified electrode: A voltammetric study

P. V. Narayana^a, T. Madhudsudhana Reddy^{*a}, P. Gopal^a and G. Ramakrishna Naidu^b

^a Electrochemical Research Laboratory, Department of Chemistry, SVU College of Sciences, Sri Venkateswara University, Tirupati- 517 502, Andhra Pradesh, India.

^b Department of Environmental Sciences, SVU College of Sciences, Sri Venkateswara University, Tirupati- 517 502, Andhra Pradesh, India.

Abstract

A facile and sensitive nanocomposite sensor was developed based on the electropolymerization of glycine (Gly) onto to the surface of glassy carbon electrode (GCE) using cyclic voltammety (CV) followed by dropcasting of multi-walled carbon nanotubes (MWCNTs). The developed nanocomposite sensor (MWCNTs/poly(Gly)/GCE) was characterized by using electrochemical impedance spectroscopy (EIS) technique. The developed nanocomposite sensor offered high catalytic activity in sensing the paracetamol (PC) individually and simultaneously in the presence of dopamine (DA) and folic acid (FA). The limit of detection (LOD) and limit of quantification (LOQ) were found to be as 5×10^{-7} M and 1.7×10^{-6} M respectively with a dynamic range from 5×10^{-7} to 1×10^{-5} M. The fabricated sensor showed good precision and accuracy with a relative standard deviation of 1.28 %. The proposed composite sensor was successfully applied towards the determination of PC in human blood serum and pharmaceutical samples.

Keywords: Paracetamol, Glycine, Cyclic voltammetry, Differential pulse voltammetry, Electrochemical impedance spectroscopy, MWCNTs

Corresponding author E-mail address: [*tmsreddysvu@gmail.com](mailto:tmsreddysvu@gmail.com), Tel.: +91-877-2289303

1.Introduction

Paracetamol (PC) or Acetaminophen (N-acetyl-p-aminophenol or 4-acetamidophenol) is non-steroidal anti-inflammatory drug and is a prominent drug that finds widespread application for its strong analgesic and antipyretic action. It is a non-carcinogenic and substitute for patients who are susceptible to aspirin and widely used for patients with headache, toothache, backache, arthritis, migraine, neuralgia, menstrual cramps and postoperative pain.¹ Usually, PC does not show any harmful side effects but hypersensitivity or overdose causes damage of liver and kidney, this leads to fatal hepatotoxicity and nephrotoxicity.²⁻⁵

The catecholamine, dopamine (DA) is a family member of neurotransmitter and exists in mammalian central nervous, cardiovascular and hormonal systems. Since its discovery, DA was playing a great deal of attention in clinical research. Due to its abnormal concentration causes numerous diseases such as Parkinson's disease and schizophrenia.⁶⁻⁸ Folic acid (pteroylglutamic acid, FA) is a water soluble vitamin (vitamin B₉). FA plays an important role in the human body, i.e. the synthesis of methionine, formation of red blood cells, differentiation of cells, single carbon group transfer reactions in metabolism (essential for synthesis of DNA and RNA) and is the precursor of the active tetrahydrofolic acid coenzyme.⁹ If a woman has enough FA in her body before and during pregnancy, it can help to prevent major birth defects of the baby's brain and spine. A woman needs 400 µg of FA every day. Deficiency of FA causes some type of anemia, psychosis and devolution of mentality.^{10,11} Due to the free radical scavenging and antioxidant activity, FA is acting as a potential agent in the prevention of cancer.¹² FA works principally in the central nervous system (CNS) and is necessary for the production of DA in the

1
2
3 CNS. Usually, PC can slow down FA from being absorbed by the body, as well as PC can also
4 increase the need for FA when taken for prolonged time.¹³ PC is likely to interfere with DA and
5 FA in their determinations. Individual determination of these compounds has been reported as
6 countless; however, their simultaneous determination of PC, DA and FA is a serious challenge
7 due to the overlapping oxidation peak potentials and is very important in the clinical and
8 pharmaceutical investigations. To the best of our knowledge, no work has been published for the
9 simultaneous determination of PC, DA and FA.
10
11
12
13
14
15
16
17
18
19

20 Carbon nanotubes (CNTs) are gifted materials in the fabrication of chemically modified
21 electrodes due to their ability to facilitate excellent electron transfer reactions¹⁴, large surface
22 area,^{15,16} good biocompatibility, high stability, modifiable side walls,¹⁷⁻²⁰ high mechanical
23 strength²¹ and high sensitivity (creates a large interfacial region).²² CNTs-based sensors provide
24 high electrocatalytic and surface anti-fouling activity.^{23,24} CNTs consist of carbon atoms with sp²
25 hybridization arranged in graphene sheets rolled up in a tube. Based on the number of walls, they
26 can be divided into single-walled carbon nanotubes (SWCNTs) and multi-walled carbon
27 nanotubes (MWCNTs).²⁵ SWCNTs have a cylindrical nanostructure, shaped by rolling up a
28 single graphite sheet into a tube whereas MWCNTs take account such type of several tubes in
29 concentric cylinders.
30
31
32
33
34
35
36
37
38
39
40
41
42

43 Various methods have been employed for the quantification of PC in pharmaceutical
44 samples and biological fluids such as flow-injection,²⁶ UV-vis spectrophotometry,²⁷ and
45 chromatographic methods.²⁸ However, these methods need more complicated procedures, costly
46 instrumentation and over analysis time when compared to electrochemical methods. In addition,
47 electrochemical methods are most suitable to examine the redox properties of newly synthesized
48 drugs. This makes an important approach in the drug discovery and in the drug analysis in their
49
50
51
52
53
54
55
56
57
58
59
60

1
2
3 dosage forms. These techniques can also solve various problems of pharmaceutical interest with
4
5 a higher degree of precision, accuracy, high sensitivity, selectivity and low background current.
6
7
8 The electrochemical techniques are also regularly used in the environmental sample analysis and
9
10 in the analysis of biologically important samples. Hence, electroanalytical methods have
11
12 received wide consideration for the determination of some biologically, pharmaceutically and
13
14 environmentally important compounds.²⁹⁻³⁷
15
16
17

18
19 The electrochemical investigation of PC at bare electrodes suffers from high over
20
21 potential and slowness of the electrode process, this leads to poor electrochemical responses. As
22
23 a result, the accuracy and precision of their determinations are extremely low in the mixed
24
25 samples. The successful route to overcome the problem of selectivity is to modify the electrode
26
27 surface, because it decreases the over potential and improves the velocity of mass transfer rate.³⁸
28
29 Recently, a huge amount of investigation has been devoted towards the development of modified
30
31 electrodes for monitoring PC in the presence of interfering substances.^{39,40} Various materials
32
33 have been used to modify the electrode surfaces, such as organic polymers,^{41,42} metal/metal
34
35 oxides-polymer⁴³ and metal-nanoparticles.^{39,40} When compared with these materials, CNTs and
36
37 its composite film based sensors show good electrical conductivity, electron transfer rate, film
38
39 forming ability, large surface area, good biocompatibility and ability in resisting interferences
40
41 from biomolecules.⁴⁴⁻⁴⁶ Hence, we have developed a highly sensitive facile nanocomposite
42
43 sensor (MWCNTs/poly(Gly)/GCE) towards the determination of PC individually and
44
45 simultaneously in the presence of DA and FA in PBS at pH 7.0. The composite was prepared
46
47 onto the surface of GCE by simple two step process, electro-polymerization of Gly followed by
48
49 drop casting of MWCNTs. The investigational results showed that the developed composite
50
51
52
53
54
55
56
57
58
59
60

1
2
3 sensor can be used for the sensing of PC concentrations in pharmaceutical preparations with
4 acceptable results.
5
6

7 8 **2. Experimental**

9 10 **2.1. Instrumentation**

11
12 CHI 660D electrochemical work station (CH Instruments, Austin, USA) was used for the
13 measurements of cyclic voltammetry, differential pulse voltammetry and electrochemical
14 impedance spectroscopy (EIS). A conventional three electrode system was employed, which
15 consists of a modified/unmodified GCE as working electrode; saturated calomel electrode (SCE)
16 as reference electrode to measure cell potentials and glassy carbon rod as an auxiliary electrode
17 to measure current. Elico U 120 pH meter combined with pH CL 51 B was used to get pH
18 values.
19
20
21
22
23
24
25
26
27
28

29 30 **2.2. Reagents**

31
32 Paracetamol from Sigma-Aldrich, India, $K_3[Fe(CN)_6]$ from Merck Specialities Pvt.
33 Limited, Mumbai. $K_4[Fe(CN)_6]$, KCl from Qualigens fine chemicals, Mumbai, Glycine from
34 Himedia Laboratories Pvt. Limited, Mumbai, Dopamine from Merck Specialities Pvt. Limited,
35 Mumbai, Folic acid from Sigma, India and Multi-walled carbon nanotubes (MWCNTs) from
36 Dropsens, Edificio CEEI, Llanera (SPAIN) was used in the present investigation. All of them
37 were used without any further purification. The stock solution of 10 mM PC was prepared and
38 stored in refrigerator, working solution was prepared by diluting the stock solution with buffer
39 solution. 0.1 M PBS was prepared from $NaH_2PO_4 \cdot 2H_2O$ and Na_2HPO_4 . All reagents are of
40 analytical grade and used without purification.
41
42
43
44
45
46
47
48
49
50
51
52
53
54
55
56
57
58
59
60

2.3. Preparation of tablet sample

650 mg of Dolo-650[®] tablet was taken and finely powdered in a mortar. The white powder was dissolved in water in 100 mL flask. The solution was shaken well to get desired concentration and then used for pharmaceutical sample studies.

2.4. Preparation of poly(Gly)/GCE

The GCE was polished on polishing pads with 0.3 and 0.05 μm of alumina slurry to get a mirror shine and cleaned thoroughly with distilled water successively. P.Raghu et al., revealed that in the preparation of polymer film coating electrodes, the positive potential scanning is the most important factor in preparing the polymer film.⁴⁷ Fig.1 shows the uninterrupted 10 CV cycles at GCE in 1mM Gly aqueous solution (pH 7.0). Initially, the scan was performed from -0.5 to 1.0 V, it was observed that no polymer film was formed on the GCE surface. However, when the window was extended from -0.5 to 1.8 V the effective polymerization was achieved. On the other hand, when the potential window was extended in negative direction the polymerization was not effective. Therefore, the window between -0.5 and 1.8 V was considered for the successful polymerization process. The film coated electrode was washed with distilled water to remove the physically adsorbed material.

(Fig.1)

2.5. Preparation of MWCNTs/GCE and MWCNTs/poly(Gly)/GCE

MWCNTs were dissolved in ethanol (1mg/ml) and ultrasonicated in a bath for 5 min to get MWCNTs dispersion. Immobilization of MWCNTs was achieved by drop casting of 5 μL of MWCNTs onto the surface of GCE and poly(Gly)GCE and dried at room temperature in the air. Hereafter the resulted electrodes were abbreviated as MWCNTs/GCE and MWCNTs/poly(Gly)/GCE respectively and were used as working electrodes.

3.Result and discussion

3.1. Electrochemical impedance study of MWCNTs/poly(Gly)/GCE

Electrochemical impedance spectroscopy (EIS) technique is a powerful and emerging tool for the study of interfacial electron transfer properties and to identify the surface nature of the electrodes. By using this technique, the impedance spectral data was recorded for bare GCE, poly(Gly)/GCE, MWCNTs/GCE and MWCNTs/poly(Gly)/GCE (in the form of Nyquist plots) in 1M KCl containing 2.5 mM $[\text{Fe}(\text{CN})_6]^{3-}/[\text{Fe}(\text{CN})_6]^{4-}$ as a redox probe at the initial potential of 0.21 V (vs SCE) with the range from 1 to 10^5 Hz (Fig.2). In the Nyquist plot, the diameter of semicircle at high frequency corresponds to the magnitude of the charge transfer resistance (R_{ct}) in the equivalent circuit. This value significantly varies based on the modification of the electrode surfaces.⁴⁸ R_{ct} and the double layer capacitance (C_{dl}) are associated with the redox behaviour of $[\text{Fe}(\text{CN})_6]^{3-/4-}$ on the active surface area of the electrodes. To calculate these values, the impedance values were fitted to the Randles equivalent circuit (Fig.2 inset), which was considered based on the features of the obtained impedance spectrum. As can be seen from the Fig.2, a semicircle with large diameter was observed with R_{ct} of 244 Ω at bare GCE. However, the diameter of semi circle diminished (R_{ct} 88.8 Ω) with the polymerization of Gly onto the GCE due to good conductivity. By drop casting of MWCNTs onto the GCE, it gave a response with low diameter of semicircle (R_{ct} 116.2 Ω) because of surface anti-fouling activity and enhanced conductivity. However, when MWCNTs was drop casted onto the poly(Gly)/GCE, the diameter of semicircle was minimum (R_{ct} 67.95 Ω). This was mainly due to the combined effect of MWCNTs and poly(Gly) film. This is the evidence for the endorsement of high charge transfer kinetics and poor charge transfer resistance at MWCNTs/poly(Gly)/GCE composite. These results confirmed the electrocatalytic activity of MWCNTs/poly(Gly)/GCE. The fitted values to the equivalence circuit for different electrodes were shown in Table.1.

(Fig.2)

(Table.1)

3.2. Electrochemical investigations of PC at MWCNTs/poly (Gly)/GCE

The electrochemical redox behavior of 1mM PC in a supporting electrolyte of 0.1M PBS at pH 7.0 was investigated using CV technique at bare GCE and different modified electrodes (Fig.3). In Fig.3, cycle-‘a’ represents the poor response of oxidation and reduction peaks with over redox potentials at bare GCE. But the redox system of PC at poly(Gly)/GCE (cycle-b) and MWCNTs/GCE (cycle-c) exhibited enhanced faradaic peak currents response with the ΔE_p of 0.080 and 0.078 V (vs SCE) respectively. However, a pair of well defined redox system with increased peak currents was observed at MWCNTs/poly(Gly)/GCE in comparison with all the three previous electrodes with the anodic and cathodic peak potentials of 0.329 and 0.270 V (vs SCE) respectively. The redox system of PC at the developed nanocomposite sensor was perfectly reversible with peak to peak separation of 0.059 V (vs SCE). In addition, the I_{pc}/I_{pa} was closer to unity and this can be considered as a decisive factor for the stability of the N-acetyl-p-benzoquinone-imine (NAPQI) formed at the surface of MWCNTs/poly(Gly)/GCE under the experimental conditions. The extraordinarily increased peak currents was due to the boost up of the electro-oxidation of PC at MWCNTs/poly(Gly)/GCE. These results noticeably show that bare GCE was modified effectively with MWCNTs/poly(Gly) composite and the MWCNTs/poly(Gly)/GCE had larger electroactive surface area in comparison with bare GCE, Poly(Gly)/GCE and MWCNTs/GCE. Furthermore, the MWCNTs/poly(Gly)/GCE can successfully facilitate the electron transfer kinetics for the electro-oxidation of PC. The schematic illustration of electro-oxidation of PC at MWCNTs/poly(Gly)/GCE can be seen in the

Scheme.1. The redox peak currents and potentials of PC at different electrodes are scheduled in Table.2.

(Scheme.1)

(Fig.3)

(Table.2)

3.3. Optimization of buffer solution pH

The DPV response of 1mM PC in 0.1 M PBS media in the range between pH 5.0 to 9.0 was investigated at MWCNTs/poly(Gly)/GCE, to assess the impact of pH on the peak currents. From Fig.4A, we can see that as the pH of the buffer was increased from 5.0 to 9.0, the anodic peak potential shifted towards negatively indicating direct involvement of protons in the rate determination step of the PC oxidation. The oxidation peak current of PC increased linearly up to pH 7.0 thereafter it was observed to be decreased dramatically. Thus, the maximum peak current was observed at pH 7.0 (Fig.4B). Therefore, pH 7.0 was chosen as an optimal pH for all the subsequent electrochemical studies in this work. Furthermore, a good linear relationship was established between the anodic peak potential and solution pH (Fig.4C) with linear regression equation of

$$E_{pa} \text{ (V)} = 0.67547 - 0.05373\text{pH} \quad (\text{R} = 0.99812).$$

From the Fig.4C, a slope value of $-0.05373 \text{ V.pH}^{-1}$ was noticed, indicating the involvement of equal number of protons and electrons in the oxidation of PC at MWCNTs/poly(Gly)/GCE. The number of electrons involved in the electro-oxidation of PC was calculated by substituting the slope value obtained from the plot of E_{pa} vs pH (Fig.4C) in the eq. (1)⁴⁹ and was found to be 2.1 (≈ 2).

$$E = E_0 - \frac{0.0591\text{pH}}{n} \dots\dots\dots(1)$$

Where 'E' is the intercept, 'E₀' is the initial potential and 'n' is the number of electrons involved in the complete reaction. The electrochemical redox mechanism of PC was represented in the Scheme.2, 'A' is an anodic peak in the positive scan direction and 'C' in the cathodic peak in the negative scan direction. This system corresponds to the transformation of PC to NAPQI and vice-versa with two-electron reversible process.

(Scheme.2)

(Fig.4A, Fig.4B & Fig.4C)

3.4. Effect of scan rate

The effect of scan rate on the peak currents was studied in the range from 0.01 to 0.15 V.s⁻¹ for 1mM PC in 0.1M PBS (pH 7.0) at MWCNTs/poly(Gly)/GCE using CV technique. As can be seen in Fig.5A, both the anodic and the cathodic peak currents were linearly allied with the square root of scan rate with the correlative coefficients (R) of 0.99922 and 0.99969 respectively.⁵⁰ These results signify that the charge transfer process was controlled by diffusion at the MWCNTs/poly(Gly)/GCE surface.⁵¹ The linear regression equations were found to be

$$I_{pa} (10^{-5}A) = 0.70534 - 34.06527 (V.s^{-1})^{1/2}$$

$$I_{pc} (10^{-5}A) = 0.52956 + 19.27343 (V.s^{-1})^{1/2}$$

In addition, the gradual change in the shape of CV at higher scan rates indicates a non-linear diffusion at more complex mass transport conditions.

(Fig.5A)

3.4.1. Apparent diffusion coefficients of PC at different electrodes

The apparent diffusion coefficients (D_{app}) of 1 mM PC in 0.1 M PBS (pH 7.0) at different modified electrodes have been estimated. D_{app} values were calculated from the Randles–Sevcik eq. (2).⁴⁹

$$I_p = (2.69 \times 10^5) n^{\frac{3}{2}} v^{\frac{1}{2}} D_{app}^{\frac{1}{2}} A C_0 \quad \dots\dots\dots (2)$$

Where 'I_p' is the peak current (A), 'n' is the number of electrons involved, 'v' is the scan rate (V s⁻¹), 'D_{app}' is the diffusion coefficient of the electroactive species (cm² s⁻¹), A is the geometrical area of electrode and C₀ is the concentration of PC (1mM).

Table.3 shows D_{app} values at bare GCE, poly(Gly)/GCE, MWCNTs/GCE and MWCNTs/poly(Gly)/GCE. As can be seen in the Fig.5B, D_{app} values were increased based on the modification. However, at MWCNTs/poly(Gly) composite modified electrode this value was two times higher than that of bare GCE. This may be due to the fast electron transfer process in the electrooxidation of PC at the boundary of the MWCNTs/poly(Gly)/GCE surface and the solutions.^{52,53} Therefore, this is also an additional evidence for the electrocatalytic activity of the MWCNTs/poly(Gly)/GCE.

(Fig.5B)

(Table.3)

3.4.2. The surface coverage concentration on MWCNTs/poly(Gly)GCE

The surface coverage concentration of developed MWCNTs/poly(Gly)/GCE was calculated using the Laviron's equation (3).⁵⁴

$$I_p = \frac{n^2 F^2 A \Gamma v}{4RT} \quad \dots\dots\dots (3)$$

Where 'n' is the number of electrons involved, 'F' is the Faraday constant (96,485 C mol⁻¹), 'Γ' is the surface coverage concentration (M.cm⁻²). 'A' is the surface area of the electrode, 'v' is the scan rate (V.s⁻¹), 'R' is the gas constant (8.314 J mol⁻¹ K⁻¹) and 'T' is the absolute temperature (300 K). The value of the surface coverage concentration (Γ) on the electrode was found to be 5.53×10⁻⁹ M.cm⁻².

3.5. Effect of PC concentration

The effect of PC concentration was examined in 0.1 M PBS (pH 7.0) at the surface of MWCNTs/poly(Gly)/GCE using DPV technique. Fig.6A illustrates that the anodic peak currents increased with the increase in concentration of PC. By plotting a graph (Fig.6-inset) between concentration of PC (10^{-7} M) and anodic peak current (10^{-7} A), an excellent linearly was connected with corresponding linear regression equation of

$$I_{pa} (10^{-7}A) = 1.02623 + 0.11245 (10^{-7}A) \quad (R = 0.99849).$$

The limit of detection (LOD) and limit of quantification (LOQ) were found to be as 5×10^{-7} M and 1.7×10^{-6} M respectively. The LOD and LOQ values were calculated by using the following equations.^{55,56}

$$LOD = 3S/M$$

$$LOQ = 10S/M$$

Where 'S' is the standard deviation of peak currents and 'M' is the slope of the working curve. The LOD and linearity range of PC at various modified electrodes were compared with our present method and are shown in Table. 4.

(Fig.6)

(Table.4)

3.6. Stability, repeatability and reproducibility of MWCNTs/poly(Gly)/GCE

In order to examine the stability of the fabricated nanocomposite sensor, 35 cycles were recorded with a gap of 2 min between each cycle in the potential range from -0.2 to 0.6 V at a scan rate of $0.05 \text{ V} \cdot \text{s}^{-1}$ for 1 mM of PC in 0.1 M PBS (pH 7.0) using CV technique (Fig.7). From Fig.7 (inset), it was observed that during these 35 cycles, there was no much interruption in the peak potentials or the peak currents of the system. This represents that the MWCNTs/poly(Gly) composite was stably adhered to the GCE surface. In terms of repeatability, a relative standard

1
2
3 deviation (RSD) of 1.28% was estimated at 1 mM of PC and indicates the composite electrode
4 does not undergo surface fouling. In addition, the reproducibility of the
5 MWCNTs/poly(Gly)/GCE was investigated by constructing four composite electrodes and these
6 were used to test in 1 mM of PC and found that there was no much change in the results.
7
8
9

10
11
12
13 (Fig.7)

14 15 **3.7. Interference study**

16
17 The selectivity of the composite sensor was investigated by detecting 100 μM of PC in
18 the presence of various interfering compounds in 0.1 M PBS at pH 7.0. The potential interfering
19 substances were selected from the group of substances commonly found with PC in
20 pharmaceuticals and biological fluids. The tolerance limit was defined as the maximum
21 concentration of the interfering substance that caused an error of less than $\pm 5\%$ for the
22 determination of PC.⁶⁸ The results show that 500 folds of ascorbic acid, dopamine, folic acid,
23 Na^+ , K^+ , NH_4^+ , Cl^- , F^- , Br^- , SO_4^{2-} doesn't affect the selectivity.
24
25
26
27
28
29
30
31
32
33
34

35 36 **3.8. Simultaneous determination and resolution of PC in the presence of DA and FA**

37
38 The determination of PC using bare GCE suffers from interference with DA and FA due
39 to their closely related oxidation potentials, however, the feasibility of the PC selective
40 determination in presence of DA and FA at MWCNTs/poly(Gly)/GCE was easier, because they
41 were well resolved with their oxidation potentials. In comparison with CV technique, the DPV
42 technique has higher current sensitivity and enhanced resolution property, due to this the DPV
43 was used to determine PC in the mixture of PC, DA and FA. The investigation was carried out
44 by varying the concentration of each individual and by keeping the concentration of remaining
45 two species constant.
46
47
48
49
50
51
52
53
54
55
56
57
58
59
60

The determination of PC in the presence of 2 μ M DA and 5 μ M FA was performed at MWCNTs/poly(Gly)/GCE with increase in the concentration of PC from 2 μ M to 35 μ M (Fig.8A). As can be seen in the Fig.8A there was no peak currents change for DA and FA however, a well resolved peak currents was observed with the increase of PC concentration. From Fig.8A (inset) it was observed that the anodic peak response was linearly connected with the concentration of PC with linear regression equation of

$$I_{pa} (10^{-7} \text{ A}) = -0.01374 + 0.09431 \text{ PC}_{\text{concentration}}(\mu\text{M}) \quad R = 0.99591$$

Similarly, the determination of DA was carried out in the presence of 4 μ M PC and 7 μ M FA with increase in the concentration of DA from 1 μ M to 35 μ M (Fig.8B). A plot between the concentration of DA and peak currents (Fig.8B (inset)) was constructed, a linear relation was observed with the linear regression equation of

$$I_{pa} (10^{-7} \text{ A}) = 3.94302 + 0.21993 \text{ DA}_{\text{concentration}}(\mu\text{M}) \quad R = 0.99846$$

FA was also determined in the presence of 2 μ M DA and 6 μ M PC with the increase in the concentration of FA from 5 μ M to 110 μ M (Fig.8C) in the same way as mentioned above. From the plot of FA concentration against the peak currents (Fig.8C(inset)), the corresponding linear regression equation was observed.

$$I_{pa} (10^{-7} \text{ A}) = 1.34555 + 0.02256 \text{ FA}_{\text{concentration}}(\mu\text{M}) \quad R = 0.99591$$

These results proved that the nanocomposite sensor was effective in simultaneous sensing of PC, DA and FA.

(Fig.8A , Fig.8B& Fig.8C)

3.9. Analytical application of pharmaceutical samples

The analytical application of the MWCNTs/poly(Gly)/GCE was validated towards the determination of PC in tablet sample (Dolo-650[®]). The tablet sample was prepared

1
2
3 approximately to get the concentration range of standard analyte. The resultant tablet solution
4
5 was analyzed in 0.1M PBS (pH 7.0) using DPV technique with a standard addition of working
6
7 analyte. The results of the analysis were given in Table.5. From these results, it can be seen that
8
9 the recovery values were satisfactory and thus, the sensing performance of
10
11 MWCNTs/poly(Gly)/GCE was extraordinary in the pharmaceutical sample.
12
13
14

15 (Table.5)
16

17 **3.10. Analytical application of pharmaceutical sample in human serum**

18
19 The electrochemical application of the present method was also verified by determining
20
21 the concentration of tablet sample (Dolo-650[®]) of PC in 10% human serum sample. The tablet
22
23 sample was prepared in the same way as discussed above. The resultant tablet solution was
24
25 spiked into the 10% human serum/PBS (pH 7.0) and analyzed using DPV technique with a
26
27 standard addition of working analyte. The results of the analysis were presented in Table.6. The
28
29 results show that the content values evaluated by the proposed method for the tablet samples
30
31 were close to the labeled content.
32
33
34
35

36 **4. Conclusions**

37
38 In the present paper, a facile and nanocomposite of MWCNTs/poly(Gly) modified GCE
39
40 was used as a sensor for the determination of PC. The developed electrochemical sensor
41
42 exhibited strong electrocatalytic activity towards PC detection and showed high sensitivity and
43
44 selectivity. The pH studies revealed that the electrooxidation of PC was two electron and two
45
46 proton process at MWCNTs/poly(Gly)/GCE. The present sensor holds great promise for the
47
48 simultaneous determination of PC, DA and FA. The sensor was also successfully used for the
49
50 determination of PC in the commercial tablet and human blood serum. Due to high stability and
51
52
53
54
55
56
57
58
59
60

1
2
3 repeatability of MWCNTs/poly(Gly)/GCE, it has the potential for the future development of
4
5 nanosensors for clinical research.
6
7
8
9

10 **Acknowledgement**

11
12 The authors are very much thankful to the authorities of Sri Venkateswara University,
13
14 Tirupati (India) for providing necessary support towards this work.
15
16
17
18
19
20
21
22
23
24
25
26
27
28
29
30
31
32
33
34
35
36
37
38
39
40
41
42
43
44
45
46
47
48
49
50
51
52
53
54
55
56
57
58
59
60

References

- 1 S. Wang, F. Xie, R. Hu, *Sens. Actuators B*, 2007, **123**, 495–500.
- 2 F. Patel, *Med. Sci. Law*, 1992, **32**, 303–310.
- 3 M.T. Olaleye, B.T.J. Rocha, *Exp. Toxicol. Pathol.* 2008, **59**, 319–327.
- 4 J. C. Roberts, H. L. Phaneuf, J. G. Szakacs, R. T. Zera, J. G. Lamb, M. R. Franklin, *Res. Toxicol.* 1998, **11**, 1274–1282.
- 5 M. Mazer, J. Perrone, *J. Med. Toxicol.*, 2008, **4**, 2–6.
- 6 C. Martin, *Chem. Br.* 1998, **34**, 40-42.
- 7 A. Heinz, H. Przuntek, G. Winterer, A. Pietzcker, *Der Nervenarzt*, 1995, **66**, 662-669.
- 8 R. M. Wightman, L. J. May, A. C. Michael, *Anal. Chem.*, 1988, **60**, 769-779.
- 9 R. L. Blakley, *The biochemistry of folic acid and related pteridines*, American Elsevier, New York, 1969.
- 10 R. M. Kok, D. E. C. Smith, J. R. Dainty, J. T. Van den Akker, , P. M. Finglas, Y. M. Smulders, C. Jacobs, K. de Meere, *Anal. Biochem.*, 2004, **326**, 129-138.
- 11 H. Karimi-Maleh, P. Biparva, M. Hatami, *Biosens. Bioelectron.*, 2013, **48**, 270–275.
- 12 Y.I. Kim, *J. Nutr. Biochem.*, 1999, **10**, 66–88.
- 13 R.T.P. Paul, A.P. McDonnell, C.B. Kelly, *Hum. Psychopharmacol. Clin. Exp.*, 2004, **19**, 477–488.
- 14 A. Mohadesi, H. Beitollahi, *Anal. Methods*, 2011, **3**, 2562–2567
- 15 F. Valentini, A. Amine, S. Orlanducci, M. L. Terranova, G. Palleschi, *Anal. Chem.*, 2003, **75**, 5413–5421.
- 16 M. Asnaashariisfahani, H. Karimi-Maleh, H. Ahmar, A. A. Ensafi, A. R. Fakhari, M. A. Khalilzadeh, F. Karimi, *Anal. Methods*, 2012, **4**, 3275–3282.

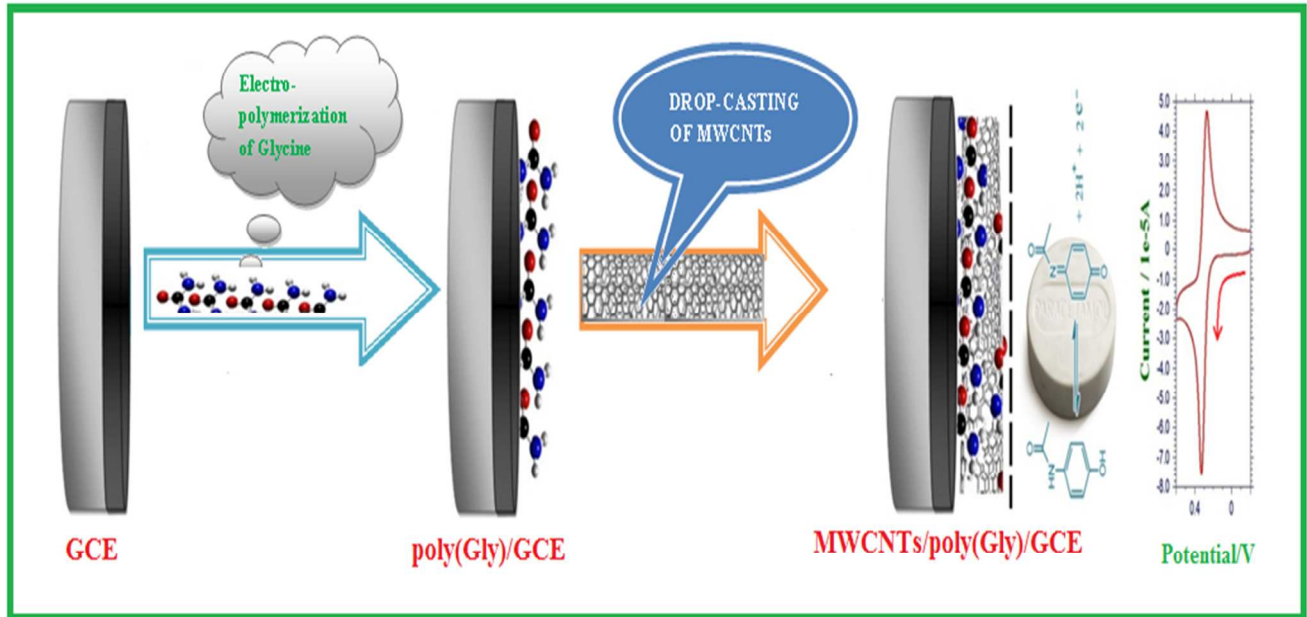
- 1
2
3
4
5
6
7
8
9
10
11
12
13
14
15
16
17
18
19
20
21
22
23
24
25
26
27
28
29
30
31
32
33
34
35
36
37
38
39
40
41
42
43
44
45
46
47
48
49
50
51
52
53
54
55
56
57
58
59
60
- 17 C. Hu, S. Hu, *Langmuir*, 2008, **24**, 8890–8897.
- 18 P.C. Chaing, W.T. Whang, *Polymer*, 2003, **44**, 2249–2254.
- 19 R. Argazzi, N.Y. M. Iha, H. Zabri, F. Odobel, C.A. Bignozzi, *Coord. Chem. Rev.*, 2004, **248**, 1299–1316.
- 20 H. Tributsch, *Coord. Chem. Rev.* 2004, **248**, 1511–1530.
- 21 A. B. Dalton, S. Collins, E. Munoz, J. M. Razal, V. H. Ebron, J. P. Ferraris, J. N. Coleman, B. G. Kim, R. H. Baughman, *Nature*, 2003, **423**, 703-703.
- 22 S. Joseph, J. F. Rusling, Y. M. Lvov, J. Friedberg, Y. M. Fuhr, *Biochem. Pharmacol.*, 2003, **65**, 1817–1826.
- 23 M. Musameh, J. Wang, A. Merkoci, Y. Lin, *Electrochem. Commun.*, 2002, **4**, 743–746.
- 24 A. A. Ensafi, M. Monsef, B. Rezaei, H. Karimi-Maleh, *Anal. Methods*, 2012, **4**, 1332–1338.
- 25 K.J. Cash, H.A. Clark, *Trends Mol. Med.*, 2010, **16**, 584-593.
- 26 N. Wangfuengkanagul, O. Chailapakul, *J. Pharm. Biomed. Anal.*, 2002, **28**, 841–847.
- 27 R.S. Andulescu, S. Mirel, R. Oprean, *J. Pharm. Biomed. Anal.*, 2000, **23**, 77–87.
- 28 W. Peng, T. Li, H. Li, E. Wang, *Anal. Chim. Acta*, 1994, **298**, 415–421.
- 29 H. Beitollahi, H. Karimi-Maleh, H. Khabazzadeh, *Anal. Chem.*, 2008, **80**, 9848–9851.
- 30 S. Tajik, M. A. Taher, H. Beitollahi, *J. Electroanal. Chem.*, 2013, **704**, 137–144.
- 31 S. Tajik, M. A. Taher, H. Beitollahi, *J. Electroanal. Chem.*, 2014, **720-721**, 134-138.
- 32 H. Beitollahi, S. Mohammadi, *Mater. Sci. Eng. C*, 2013,**33**, 3214–3219.
- 33 H. Beitollahi, M. Mostafavi, *Electroanalysis*, 2014, **26**, 1090–1098.
- 34 A. Mohadesi, H. Beitollahi, *Anal. Methods*, 2011, **3**, 2562–2567.
- 35 S. Mohammadi, H. Beitollahi, A. Mohadesi, *Sens. Lett.* 2013,**11**, 388-394

- 1
2
3 36 M. Elyasi, M.A. Khalilzadeh, H. Karimi-Maleh, *Food Chem.*, 2013, **141**, 4311–4317
4
5
6
7 37 T. Tavana, M. A. Khalilzadeh, H. Karimi-Maleh, A. A. Ensafi, H. Beitollahi, D. Zareyee, *J.*
8
9
10
11
12 38 H. Karimi-Maleh, M. Moazampour, H. Ahmar, H. Beitollahi, A. A. Ensafi, *Measurement*
13
14 2014, **51**, 91–99.
15
16 39 M. M. Ardakani, H. Beitollahi, M. K. Amini, F. Mirkhalaf, M. A. Alibeik, *Sens. Actuators B*,
17
18 2010, **151**, 243–249.
19
20
21 40 N. F. Atta, A. Galal, F. M. A. Attia, S. M. Azab, *J. Mater. Chem.*, 2011, **21**, 13015–13024.
22
23 41 A.M. Yu, H.-L. Zhang, H.-Y. Chen, *Electroanalysis*, 1997, **9**, 788-790.
24
25 42 Y. Li, X. Liu, W. Wei, *Electroanalysis*, 2011, **23**, 2832-2838.
26
27 43 S. Reddy, B.E.K. Swamy, H.N. Vasan, H. Jayadevappa, *Anal. Methods*, 2012, **4**, 2778-2783.
28
29 44 H. Karimi-Maleh, F. Tahernejad-Javazmi, M. Daryanavard, H. Hadadzadeh, A.A. Ensafi, M.
30
31 Abbasghorbani, *Electroanalysis*, 2014, **26**, 962 – 970.
32
33 45 H. Beitollah, M. Goodarzian, M. A. Khalilzadeh, H. Karimi-Maleh, M. Hassanzadeh, M.
34
35 Tajbakhsh, *J. Mol. Liq.*, 2012, **173**, 137–143.
36
37 46 R. Moradi, S. A. Sebt, H. Karimi-Maleh, R. Sadeghi, F. Karimi, A. Baharie, H. Arabi, *Phys.*
38
39
40
41
42
43
44
45 47 P. Raghu, T. Madhusudana Reddy, P. Gopal, K. Reddaiah, N.Y. Sreedhar, *Enzyme Microb.*
46
47
48
49
50 48 Y. J. Liu, F. Yin, Y. M. Long, Z. H. Zhang, S. Z. Yao, *J. Colloid Interface Sci.*, 2003, **258**, 75–
51
52 81.
53
54 49 A. J. Bard and L. R. Faulkner, *Electrochemical Methods: Fundamentals and Applications*,
55
56 John Wiley, New York, 2001.
57
58
59
60

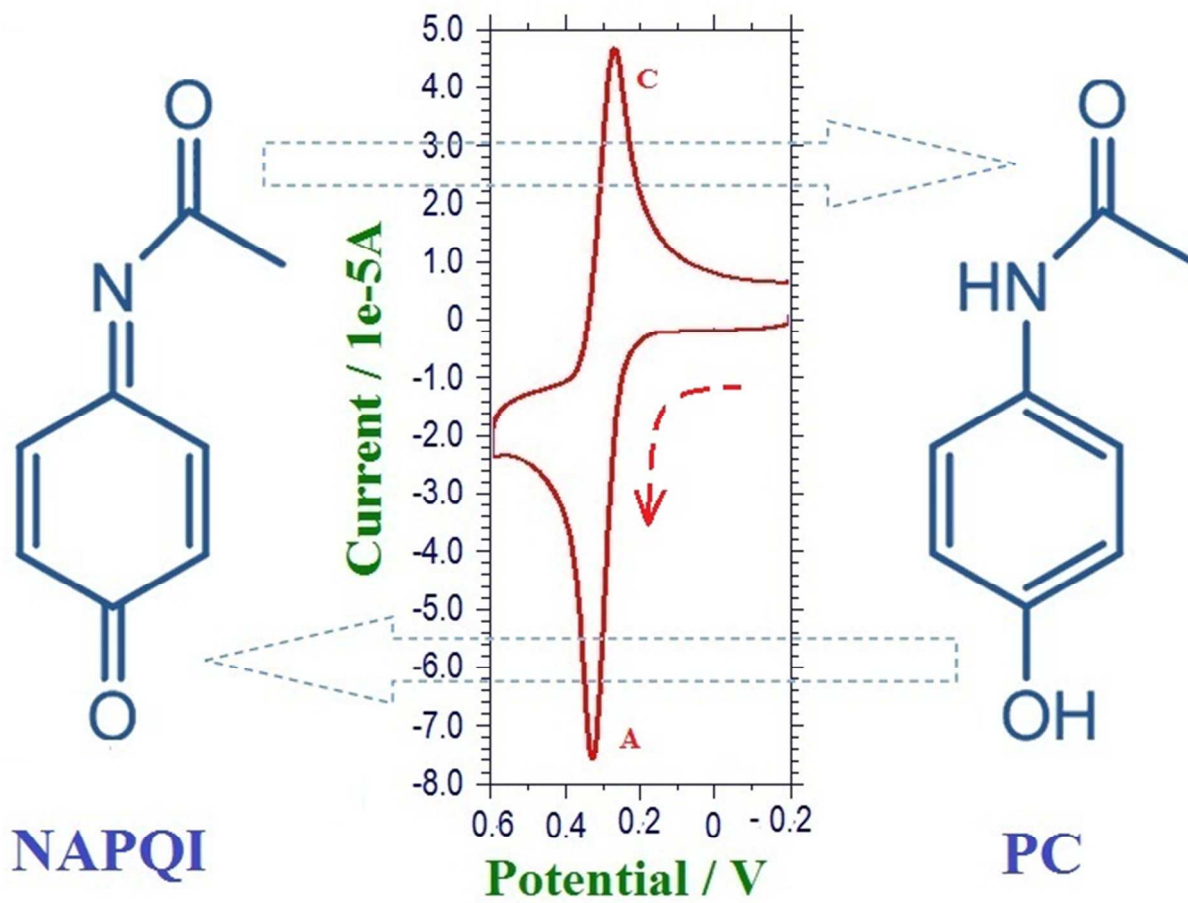
- 1
2
3
4 50 J.B. Raoof, R. Ojani, Z. Mohammadpour, , *Int. J. Electrochem. Sci.*, 2010, **5**, 177-188.
5
6 51 P. Raghu, B. E. K. Swamy, T. Madhusudana Reddy, B. N. Chandrashekar, K. Reddaiah,
7
8 *Bioelectrochemistry*, 2012, **83**, 19–24.
9
10 52 Q. Wan, N. Yang, X. Zou, H. Zhang, B. Xu, *Talanta*, 2002, **55**, 459–467.
11
12 53 V.S. Vasantha, S.-M. Chen, *J. Electroanal. Chem.*, 2006, **592**, 77–87.
13
14 54 E. Laviron. *J. Electroanal. Chem.*, 1979, **100**, 263–270.
15
16 55 K. Reddaiah, T. Madhusudana Reddy, P. Raghu, *J. Electroanal. Chem.*, 2012, **682**, 164–171
17
18 56 T. Madhusudana Reddy, M. Sreedhar, S. J. Reddy, *J. Pharm. Biomed. Anal.*, 2003, **31**, 811–
19
20 818.
21
22 57 I. Noviadri, R. Rakhmana, *Int. J. Electrochem. Sci.*, 2012, **7**, 4479 - 4487.
23
24 58 H. Beitollahi, A. Mohadesi, S. Mohammadi, A. Akbari, *Electrochim. Acta*, 2012, **68**, 220-226.
25
26 59 R. N. Goyal, V. K. Gupta, M. Oyama, N. Bachheti, *Electrochem. Commun.*, 2005, **7**, 803-807.
27
28 60 J. B. Raoof, M. Baghayeri, R. Ojani, *Colloid Surf. B*, 2012, **95**, 121-128.
29
30 61 R. N. Goyal, S. P. Singh, *Electrochim. Acta*, 2006, **51**, 3008–3012.
31
32 62 S. A. Kumar, C. F. Tang, S. M. Chen, *Talanta*, 2008, **76**, 997-1005.
33
34 63 M. Li, L. Jing, *Electrochim. Acta*, 2007, **52**, 3250-3257.
35
36 64 C. Cofan, C. Radovan, *Sensors*, 2008, **8**, 3952-3969.
37
38 65 J.-M. Zen, Y.-S. Ting, *Anal. Chim. Acta*, 1997, **342**, 175-180.
39
40 66 W.-Y. Su, S.-H. Cheng, *Electroanalysis*, 2010, **22**, 707–714.
41
42 67 Z. A. Alothman, N. Bukhari, S. M. Wabaidur, S. Haider, *Sens. Actuators B*, 2010,**146**, 314–
43
44 320.
45
46 68 H. K. -Maleh, F. T. –Javazmi, A. A. Ensafi, R. Moradi, S. Mallakpour, H. Beitollahi, *Biosens.*
47
48 *Bioelectron.*, 2014, **60**, 1–7.
49
50
51
52
53
54
55
56
57
58
59
60

Schemes & Figures

Schemes :



Scheme.1



Scheme.2

1
2
3
4
5
6
7
8
9
10
11
12
13
14
15
16
17
18
19
20
21
22
23
24
25
26
27
28
29
30
31
32
33
34
35
36
37
38
39
40
41
42
43
44
45
46
47
48
49
50
51
52
53
54
55
56
57
58
59
60

Figures:

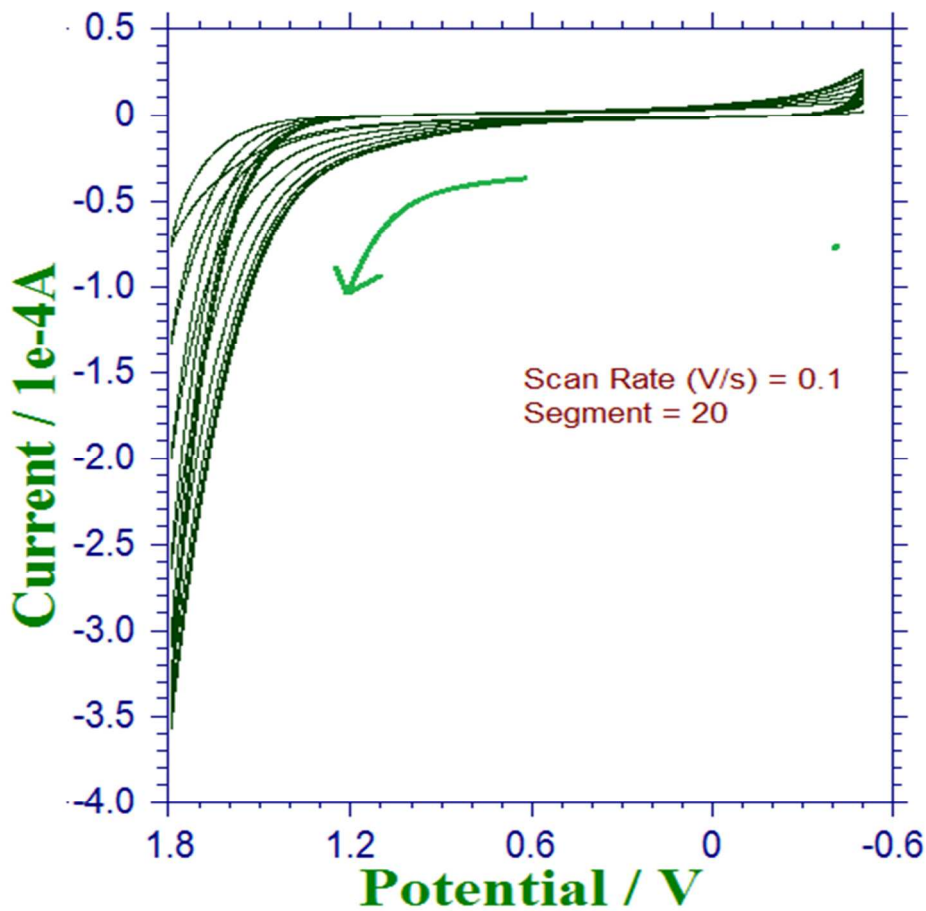


Fig.1

1
2
3
4
5
6
7
8
9
10
11
12
13
14
15
16
17
18
19
20
21
22
23
24
25
26
27
28
29
30
31
32
33
34
35
36
37
38
39
40
41
42
43
44
45
46
47
48
49
50
51
52
53
54
55
56
57
58
59
60

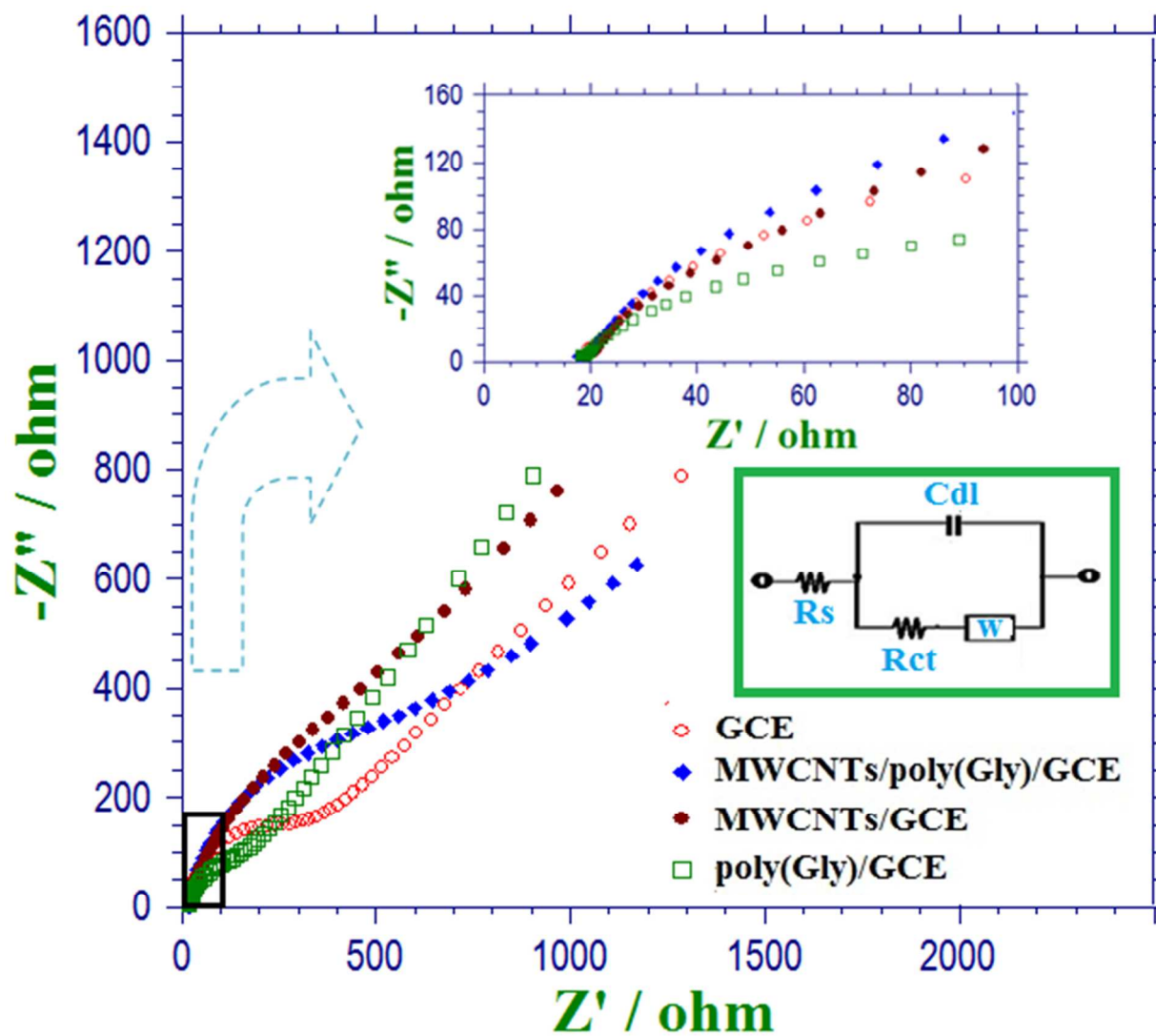


Fig.2

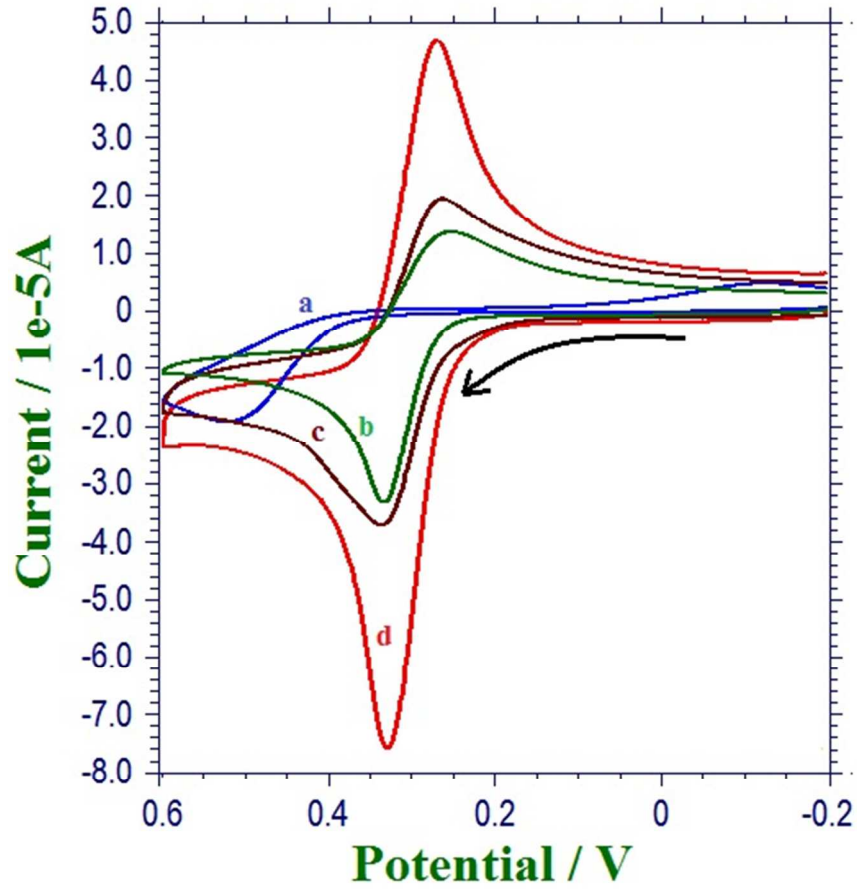


Fig.3

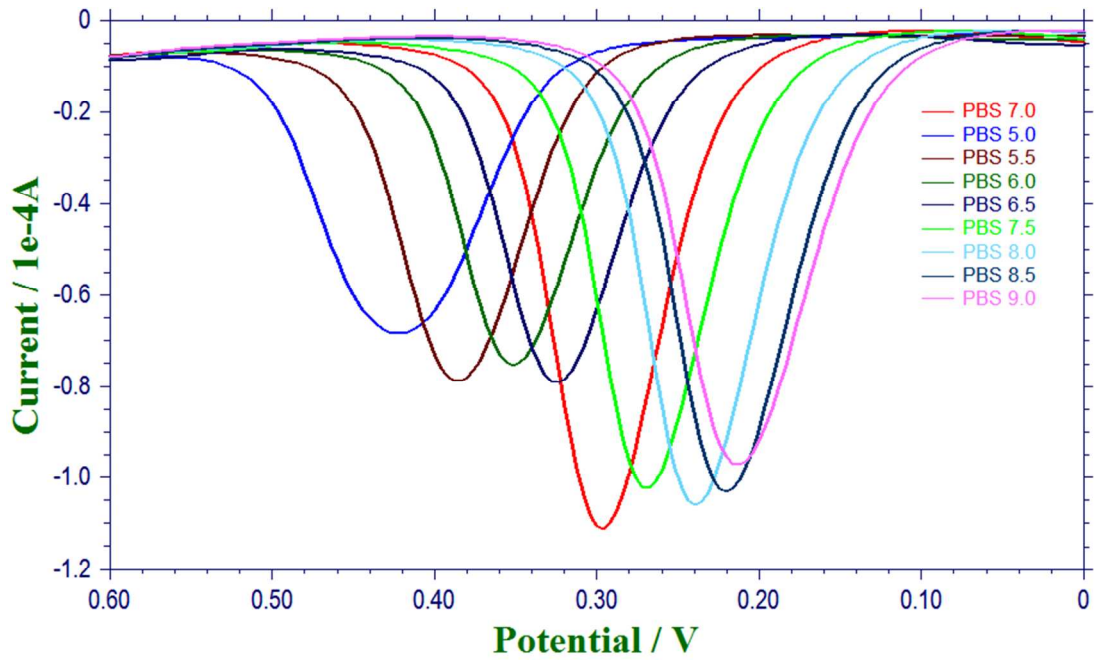


Fig.4A

1
2
3
4
5
6
7
8
9
10
11
12
13
14
15
16
17
18
19
20
21
22
23
24
25
26
27
28
29
30
31
32
33
34
35
36
37
38
39
40
41
42
43
44
45
46
47
48
49
50
51
52
53
54
55
56
57
58
59
60

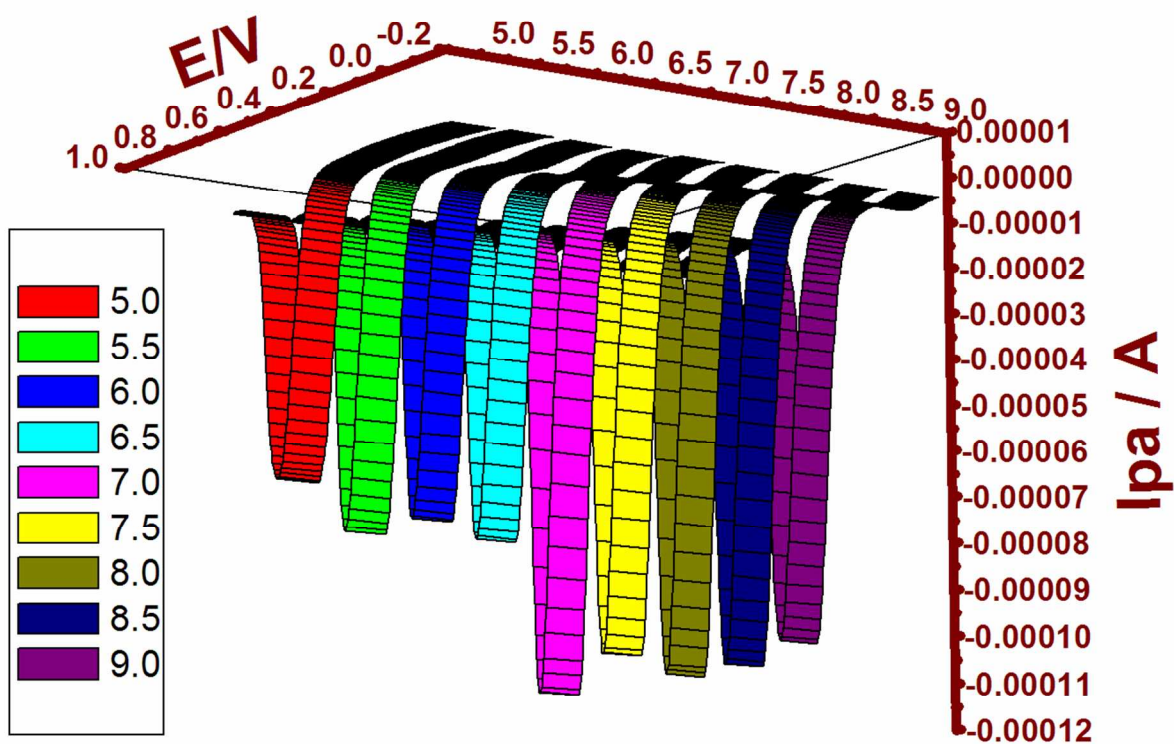


Fig.4B

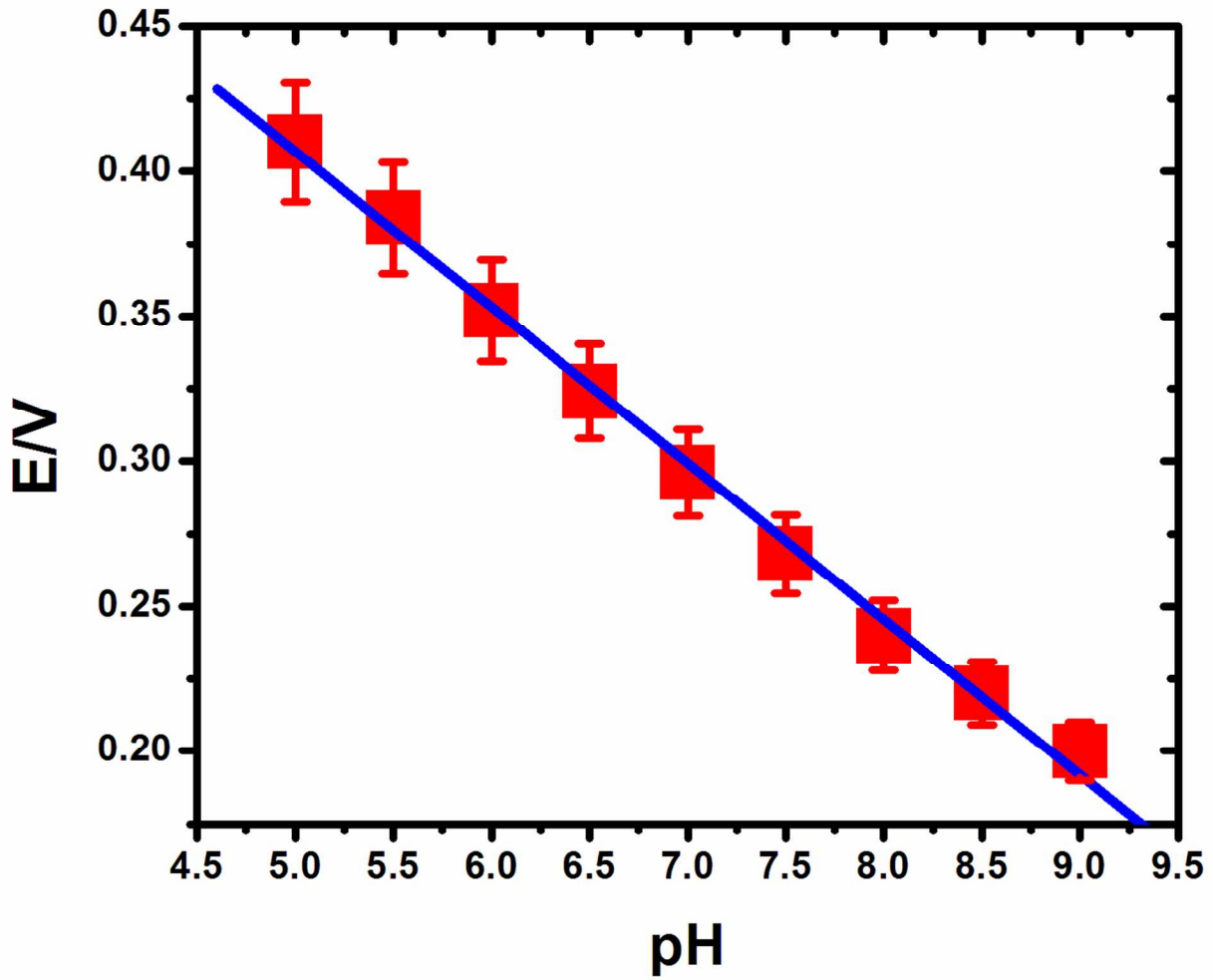


Fig.4C

1
2
3
4
5
6
7
8
9
10
11
12
13
14
15
16
17
18
19
20
21
22
23
24
25
26
27
28
29
30
31
32
33
34
35
36
37
38
39
40
41
42
43
44
45
46
47
48
49
50
51
52
53
54
55
56
57
58
59
60

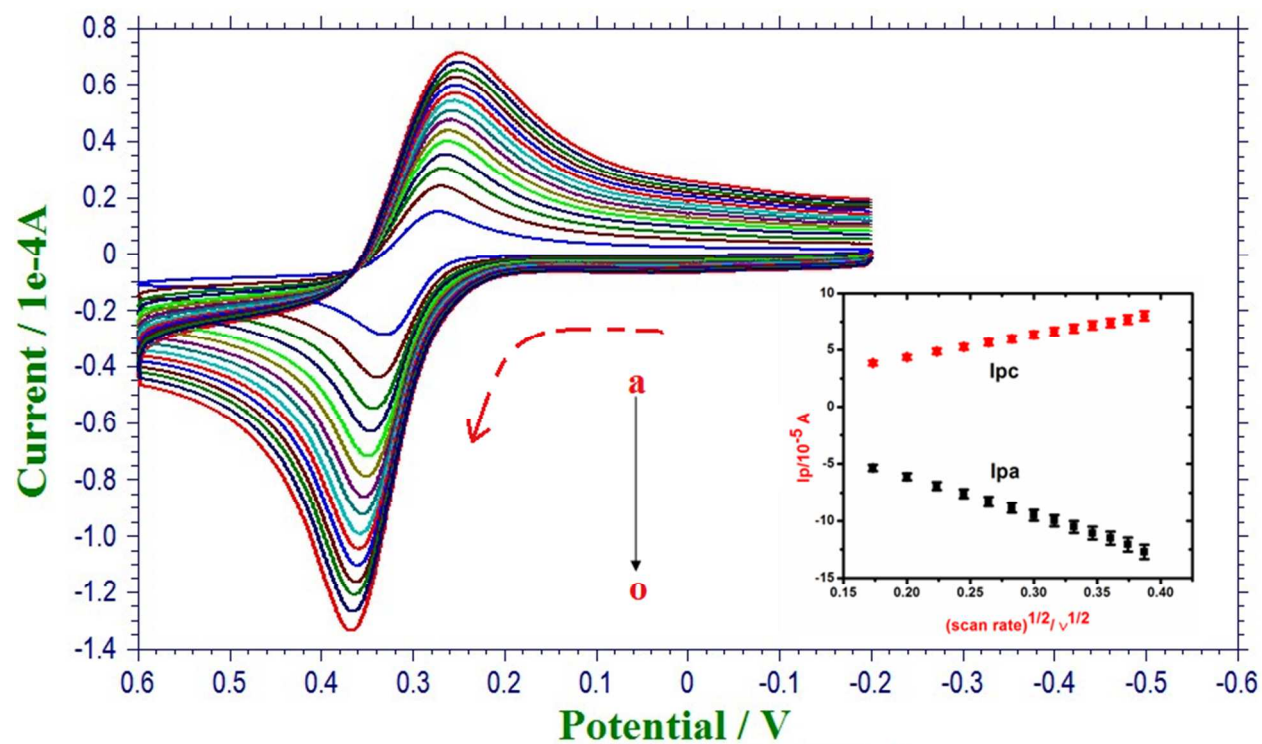


Fig.5A

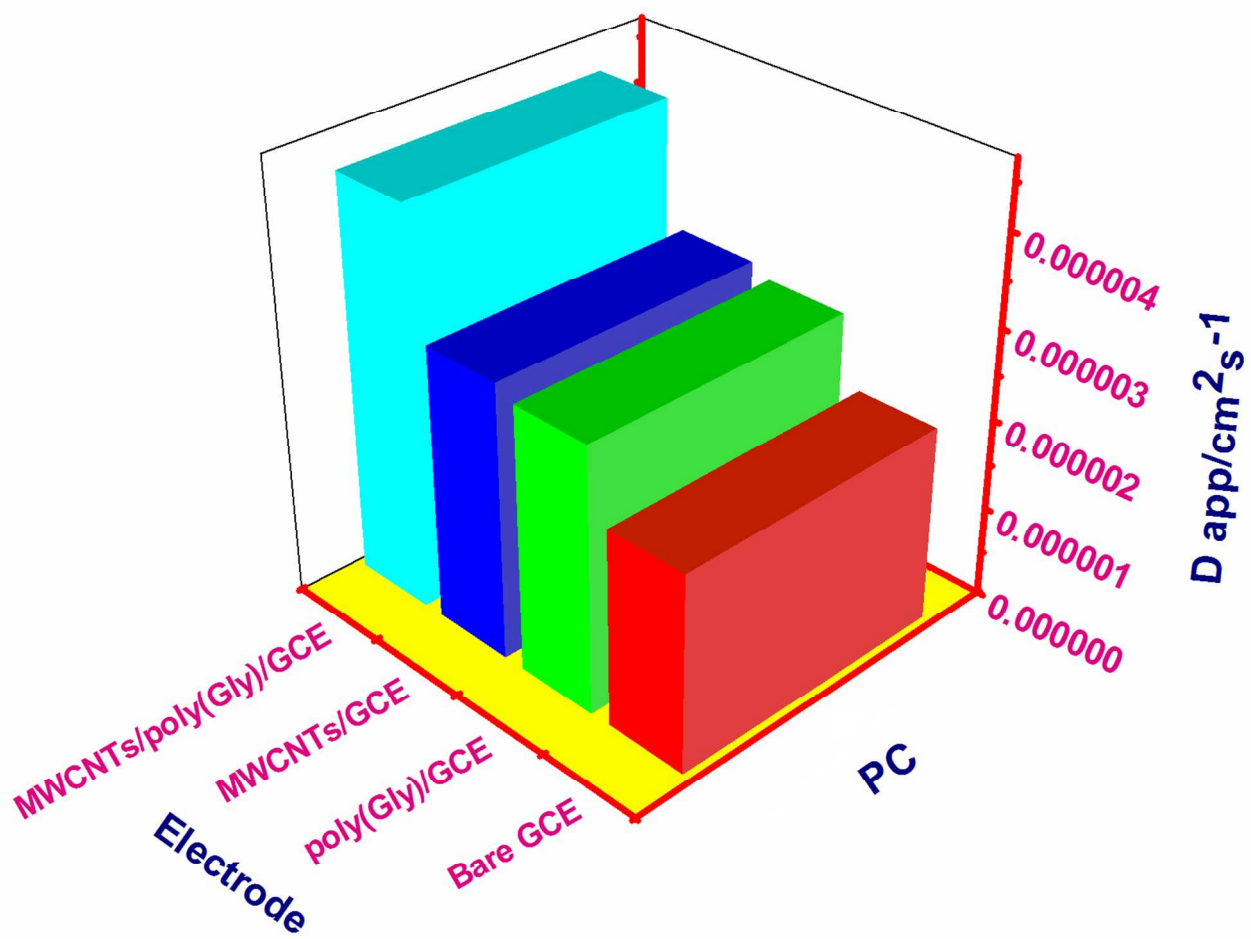


Fig.5B

1
2
3
4
5
6
7
8
9
10
11
12
13
14
15
16
17
18
19
20
21
22
23
24
25
26
27
28
29
30
31
32
33
34
35
36
37
38
39
40
41
42
43
44
45
46
47
48
49
50
51
52
53
54
55
56
57
58
59
60

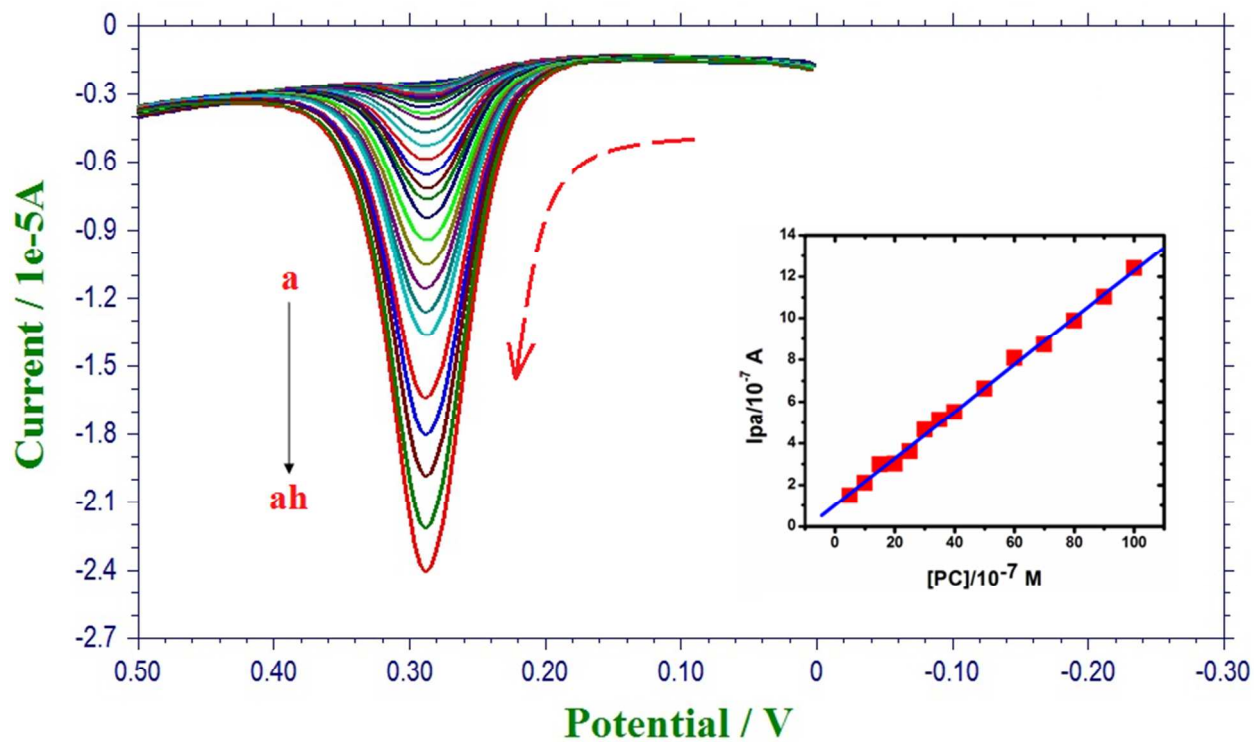


Fig.6

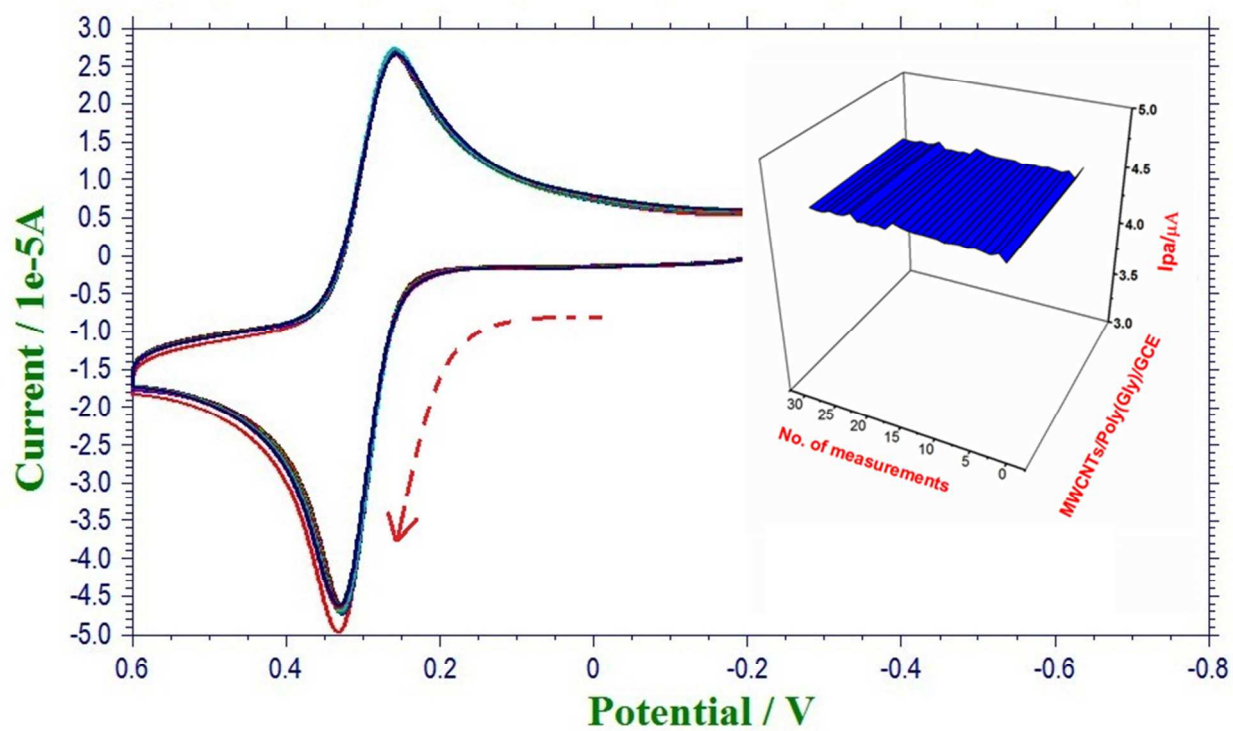


Fig.7

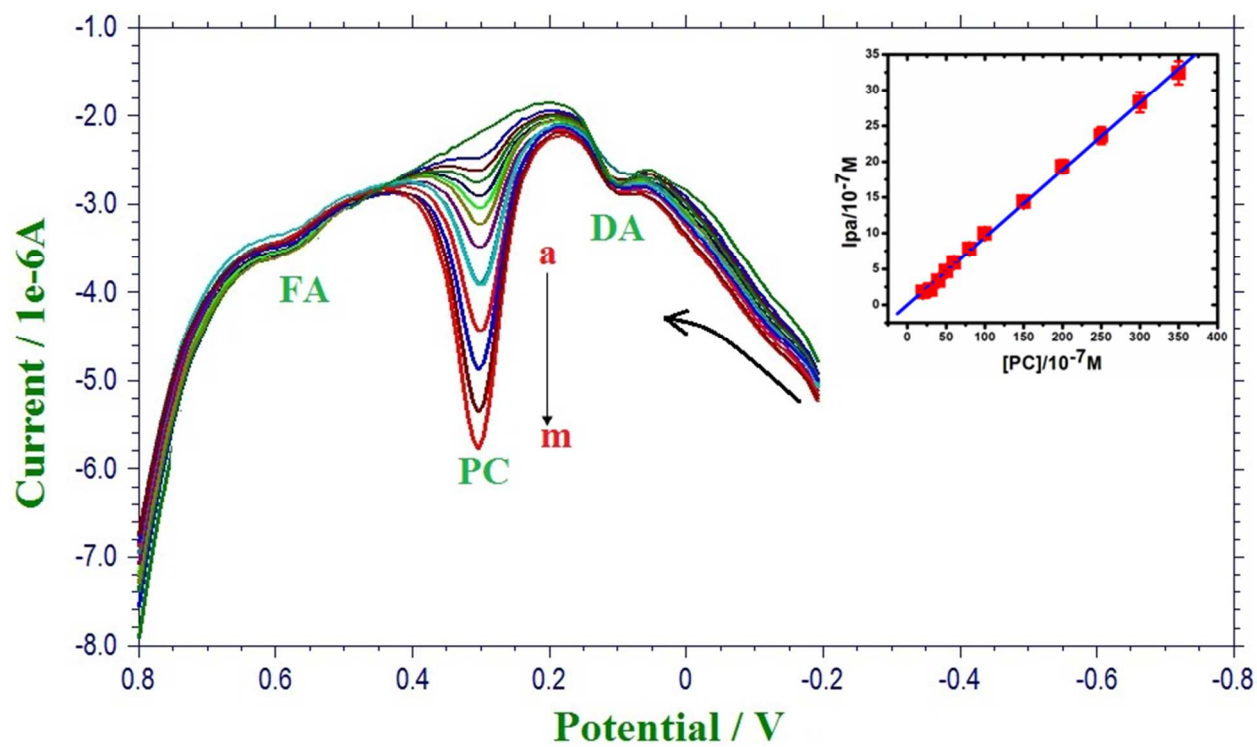


Fig.8A

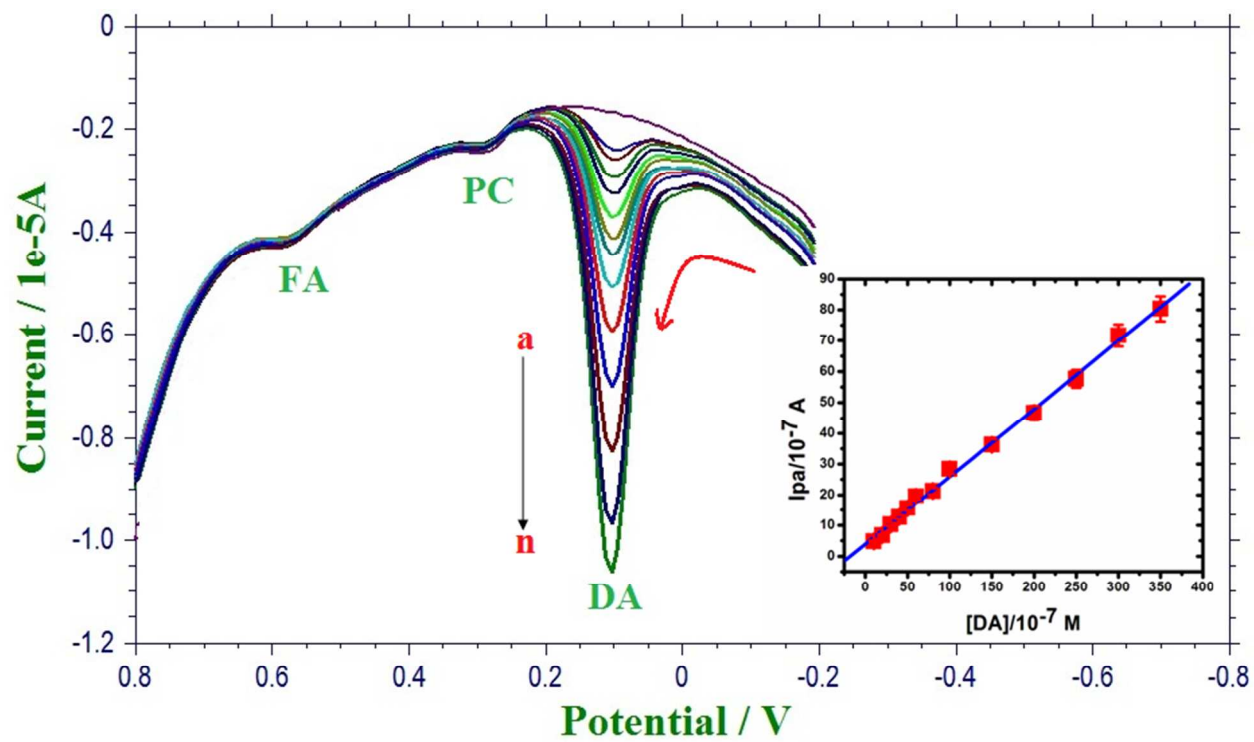


Fig.8B

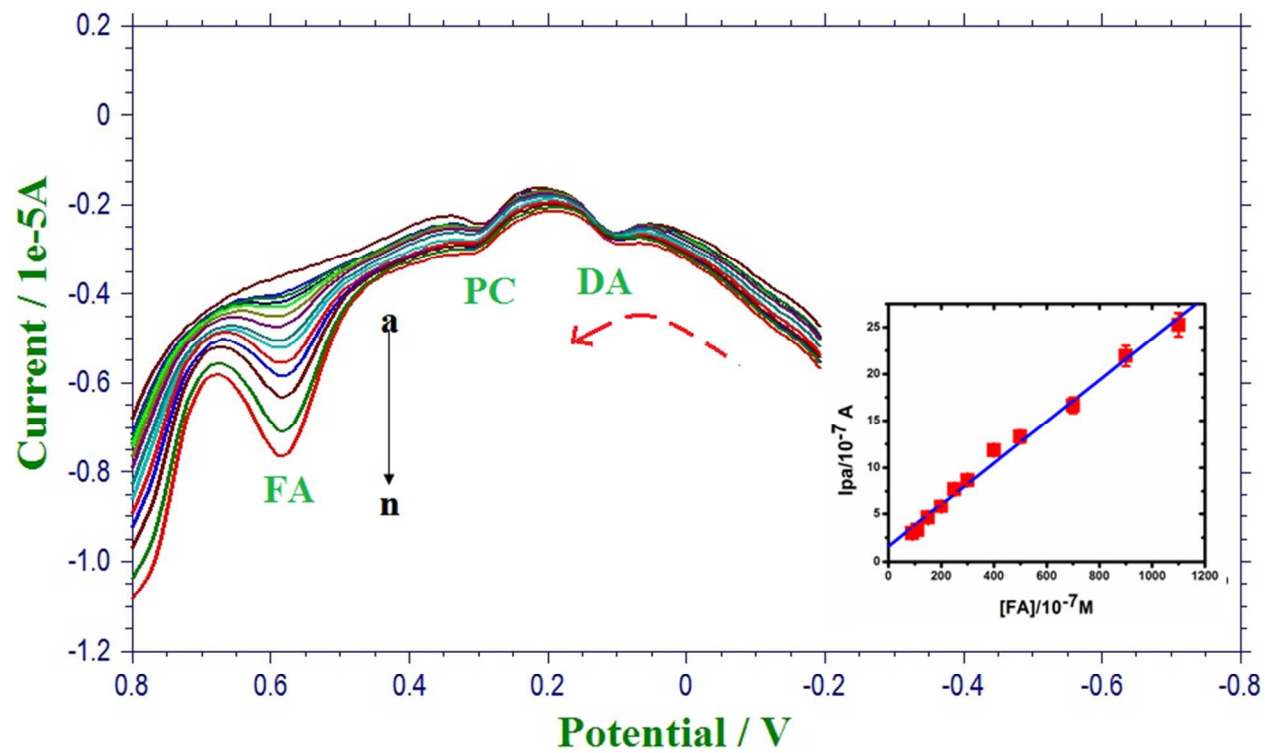


Fig.8C

Schemes & Figure Captions:

Scheme.1 The illustration of electrode preparation and mechanism of MWCNTs/poly(Gly)/GCE towards the determination of PC.

Scheme.2 The electrochemical redox mechanism of PC at MWCNTs/poly(Gly)/GCE.

Fig.1. Cyclic voltammograms for the electrochemical polymerization of Glycine at GCE.

Fig.2. EIS spectrum of 1 M KCl containing 2.5mM $[\text{Fe}(\text{CN})_6]^{-3/4}$ at different electrodes, inset- equivalent circuit to MWCNTs/poly(Gly)/GCE.

Fig.3. Cyclic voltammograms for the electrochemical response of 1mM PC at (a) bare GCE, (b) poly(Gly)/GCE, (c) MWCNTs/GCE and (d) MWCNTs/poly(Gly)/GCE in 0.1M PBS of pH 7.0 at a scan rate of $0.05 \text{ V}\cdot\text{s}^{-1}$

Fig.4(A). Differential pulse voltammograms obtained at MWCNTs/poly(Gly)/GCE in 0.1 M PBS solution at different pH values.

Fig.4(B). A 3 dimensional plot of PC oxidation peak current at various pH.

Fig.4(C). A plot between PC oxidation peak potential vs pH of PBS.

Fig. 5(A). Cyclic voltammograms of PC at MWCNTs/poly(Gly)/GCE in 0.1 M PBS solution of pH 7.0 at different scan rates (a to o, $0.01\text{--}0.15 \text{ V}\cdot\text{s}^{-1}$). **inset-** Calibration plots for the redox peak currents vs the square root of scan rate.

Fig. 5(B). 3 dimensional plot of apparent diffusion coefficients of PC at different electrodes.

Fig.6. Differential pulse voltammograms of PC for the different concentrations in PBS at pH 7.0

(a) $5 \times 10^{-7} \text{ M}$ (b) $1 \times 10^{-6} \text{ M}$ (c) $1.5 \times 10^{-6} \text{ M}$ (d) $2 \times 10^{-6} \text{ M}$ (e) $2.5 \times 10^{-6} \text{ M}$ (f) $3 \times 10^{-6} \text{ M}$ (g) $3.5 \times 10^{-6} \text{ M}$ (h) $4 \times 10^{-6} \text{ M}$ (i) $5 \times 10^{-6} \text{ M}$ (j) $6 \times 10^{-6} \text{ M}$ (k) $7 \times 10^{-6} \text{ M}$ (l) $8 \times 10^{-6} \text{ M}$ (m) $9 \times 10^{-6} \text{ M}$ (n) $1 \times 10^{-5} \text{ M}$ (o) $1.2 \times 10^{-5} \text{ M}$ (p) $1.4 \times 10^{-5} \text{ M}$ (q) $1.6 \times 10^{-5} \text{ M}$ (r) $2 \times 10^{-5} \text{ M}$ (s) $2.5 \times 10^{-5} \text{ M}$ (t) $3 \times 10^{-5} \text{ M}$

1
2
3 (u) 3.50×10^{-5} M (v) 4×10^{-5} M (w) 4.5×10^{-5} M (x) 5×10^{-5} M (y) 6×10^{-5} M (z) 7×10^{-5} M (aa) $8 \times$
4
5 10^{-5} M (ab) 9×10^{-5} M (ac) 1×10^{-4} M (ad) 1.2×10^{-4} M (ae) 1.4×10^{-4} M (af) 1.6×10^{-4} M (ag) $1.8 \times$
6
7 10^{-4} M (ah) 2×10^{-4} M; **inset**-Calibration plot of PC concentration.

8
9
10 **Fig.7** Cyclic voltammograms for 35 parallel cycles of 1mM PC in 0.1M PBS solution of pH 7.0
11
12 at a scan rate of 0.05 V.s^{-1} ; **inset**- A plot of 35 parallel cycles of CVs vs. I_{pa} .

13
14 **Fig. 8(A)** Differential pulse voltammograms obtained for determination of PC, in the presence of
15
16 2×10^{-6} M DA and 5×10^{-6} M FA at MWCNTs/poly(Gly)/GCE. Concentration of PC: (a) without
17
18 PC (b) 2×10^{-6} M (c) 3×10^{-6} M (d) 4×10^{-6} M (e) 5×10^{-6} M (f) 6×10^{-6} M (g) 8×10^{-6} M (h) 1×10^{-5} M
19
20 (i) 1.5×10^{-5} M (j) 2×10^{-5} M (k) 2.5×10^{-5} M (l) 3×10^{-5} M (m) 3.5×10^{-5} M; **inset**- Calibration plot of
21
22 PC determination.
23
24
25
26

27 **Fig. 8 (B)** Differential pulse voltammograms obtained for determination of DA, in presence of
28
29 4×10^{-6} M PC and 7×10^{-6} M FA at MWCNTs/poly(Gly)/GCE. Concentration of DA : (a) without
30
31 DA (b) 1×10^{-6} M (c) 2×10^{-6} M (d) 3×10^{-6} M (e) 4×10^{-6} M (f) 5×10^{-6} M (g) 6×10^{-6} M (h) 8×10^{-6} M
32
33 (i) 1×10^{-5} M (j) 1.5×10^{-5} M (k) 2×10^{-5} M (l) 2.5×10^{-5} M (m) 3×10^{-5} M (n) 3.5×10^{-5} M; **inset**-
34
35 Calibration plot of DA determination.
36
37
38

39 **Fig.8 (C)** Differential pulse voltammograms obtained for determination of FA, in presence of
40
41 2×10^{-6} M DA and 6×10^{-6} M PC at MWCNTs/poly(Gly)/GCE. Concentration of FA : (a) without
42
43 FA (b) 5×10^{-6} M (c) 7×10^{-6} M (d) 9×10^{-6} M (e) 1.1×10^{-5} M (f) 1.5×10^{-5} M (g) 2×10^{-5} M (h)
44
45 2.5×10^{-5} M (i) 3×10^{-5} M (j) 4×10^{-5} M (k) 5×10^{-5} M (l) 7×10^{-5} M (m) 9×10^{-5} M (n) 1.1×10^{-4} M;
46
47 **inset**-Calibration plot of FA determination.
48
49
50
51
52
53
54
55
56
57
58
59
60

Tables

Table .1: Electrochemical impedance spectroscopy response at different electrodes

Electrode	Rs ^a (Ω)	Cdl	Rct (Ω)	W ^b
GCE	21.43	5.367×10 ⁻⁷	244.3	0.0002297
poly(Gly)/GCE	19.36	2.378×10 ⁻⁶	88.8	0.0003635
MWCNTs/GCE	20.06	8.911×10 ⁻⁶	116.2	0.0002954
MWCNTs/poly(Gly)/GCE	17.81	1.7×10 ⁻⁵	67.95	0.0004986

^aSolution resistance^bWarburg impedance

Table .2: Comparison between the electroactivity of GCE modified electrodes towards the electro-oxidation of PC

Electrode	I _{pa} /A	E _{pa} /V	E _{pc} /V	ΔE _p /V	Enhancement in sensitivity ^a
GCE	-1.784×10 ⁻⁵	0.522	-0.123	123.522	1.00
poly(Gly)/GCE	-3.239×10 ⁻⁵	0.334	0.254	0.080	1.81
MWCNTs/GCE	-3.504×10 ⁻⁵	0.337	0.263	0.078	1.96
MWCNTs/poly(Gly)/GCE	-7.334×10 ⁻⁵	0.329	0.270	0.059	4.11

^aNormalized to the current obtained at GCE

Table.3: Apparent diffusion coefficient values of PC at different electrodes

S.No.	Electrode	D_{app} Values(cm^2s^{-1})
1	Bare GCE	2.161×10^{-6}
2	poly(Gly)/GCE	2.912×10^{-6}
3	MWCNTs/GCE	3.028×10^{-6}
4	MWCNTs/poly(Gly)/GCE	4.382×10^{-6}

Table.4: Comparison of the efficiency of some modified electrodes used in the electro-oxidation of PC.

Electrode	Method	LOD (M)	Dynamic Range (M)	Reference
MWCNTs/paste electrode	SWV	1.1×10^{-6}	1×10^{-5} - 1×10^{-4}	57
5-amino-3',4'- dimethyl-biphenyl- 2-ol-CNT/paste electrode	SWV	2.0×10^{-7}	4×10^{-7} - 9×10^{-4}	58
ITO/nAu	DPV	0.18×10^{-6}	0.2×10^{-6} - 15×10^{-4}	59
Nano Pt-MWCNT/ paste electrode	DPV	1.7×10^{-7}	5×10^{-7} - 1×10^{-4}	60
GCE/C ₆₀	DPV	5×10^{-5}	5×10^{-5} - 15×10^{-4}	61
Poly(acid yellow 9)-TiO ₂ /GCE	DPV	2×10^{-6}	1.2×10^{-5} - 1.2×10^{-4}	62
GCE/PANI-MWCNTs	SWV	0.25×10^{-6}	1×10^{-6} - 1×10^{-4}	63
GCE/C-Ni	DPV	0.6×10^{-6}	2×10^{-6} - 23×10^{-5}	1
Boron-Doped Diamond Electrode	Chrono amp	1.42×10^{-6}	-----	64
GCE/Nafion/RuO	SWV	1.2×10^{-6}	5×10^{-6} - 250×10^{-6}	65
SPE/PEDOT	DPV	1.39×10^{-6}	4×10^{-6} - 400×10^{-6}	66
f-MWCNTs/GCE	DPV	0.6×10^{-6}	3×10^{-6} - 3×10^{-4}	67
MWCNTs/poly(Gly)/GCE	DPV	5×10^{-7}	5×10^{-7} to 1×10^{-5}	Present work

Table.5: Determination of PC in pharmaceutical preparations.

Sample	Added (μM)	Found (μM)	Recovery (%)	Bias (%)
Dolo-650 [®]	10	10.07	100.7	+0.7
	20	20.21	101.05	+1.05
	30	29.76	99.2	-0.8

Table.6: Determination of PC in human serum.

Sample	Added (μM)	Found (μM)	Recovery (%)	Bias (%)
Serum	10	10.08	100.8	+0.8
	20	20.33	101.65	+1.65